

## Supplementary Data

# Rational design of MXene@TiO<sub>2</sub> nanoarray enabling dual lithium-polysulfides chemisorption towards high-performance lithium-sulfur batteries

Sheng-You Qiu,<sup>a,1</sup> Chuang Wang,<sup>a,1</sup> Zai-Xing Jiang,<sup>a</sup> Li-Su Zhang,<sup>b</sup> Liang-Liang Gu,<sup>a</sup> Ke-Xin Wang,<sup>a</sup> Jian Gao,<sup>b</sup> Xiao-Dong Zhu<sup>\*a,b</sup> and Gang Wu<sup>\*c</sup>

- a. School of Chemistry and Chemical Engineering, Harbin Institute of Technology, Harbin, 150001, China. E-mail: zxd9863@163.com.
- b. State Key Laboratory Base of Eco-Chemical Engineering, College of Chemical Engineering, Qingdao University of Science & Technology, Qingdao, 266042, China. E-mail: xiao-dong\_zhu@qust.edu.cn.
- c. Department of Chemical and Biological Engineering, University at Buffalo, The State University of New York, Buffalo, New York 14260, USA. E-mail: gangwu@buffalo.edu.

1. S.-Y. Qiu and C. Wang contributed equally to this work.

**Supplementary Figures and Tables**

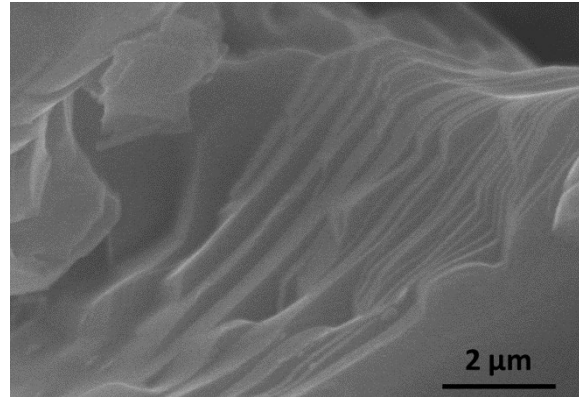


**Fig. S1 SEM image of MAX precursor.**

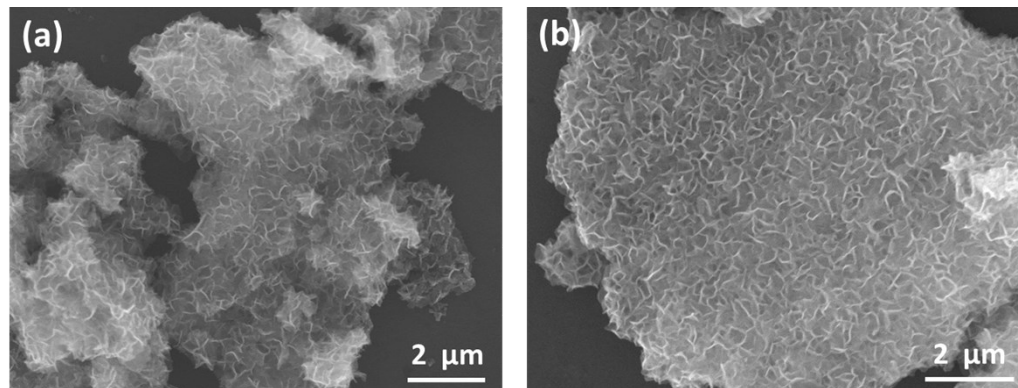


**Fig. S2 Overall SEM images of MXene@TiO<sub>2</sub> nanoarray.**

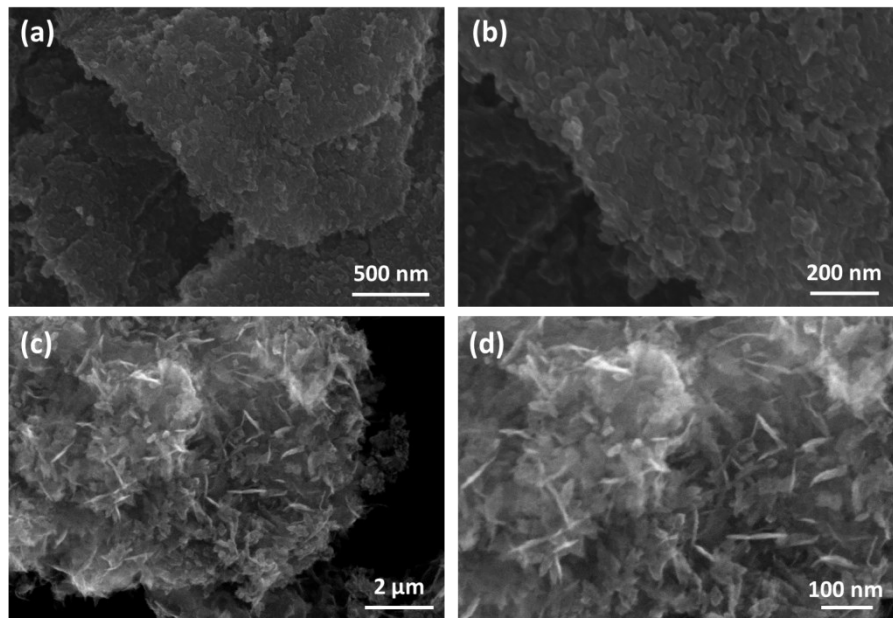


**Fig. S3** SEM images of MXene@TiO<sub>2</sub> composites with different inputs of titanium(IV) isopropoxide: (a, b) 0.6 mL; (c, d) 1.4 mL.

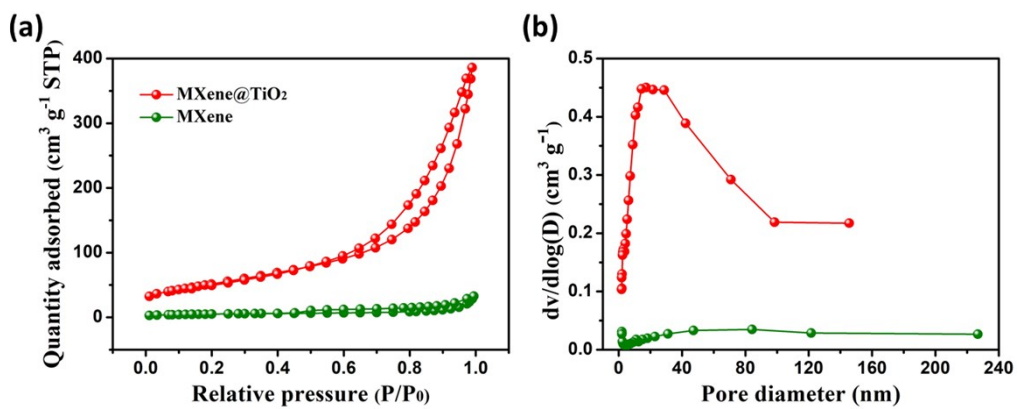


**Fig. S4** (a) Nitrogen adsorption-desorption isotherms and (b) pore size distributions of MXene@TiO<sub>2</sub> nanoarray and individual MXene nanosheets.

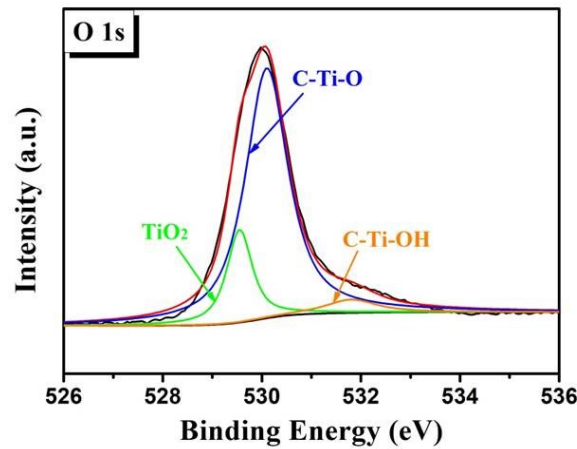


Fig. S5 O 1s XPS spectrum of MXene@TiO<sub>2</sub> nanoarray.

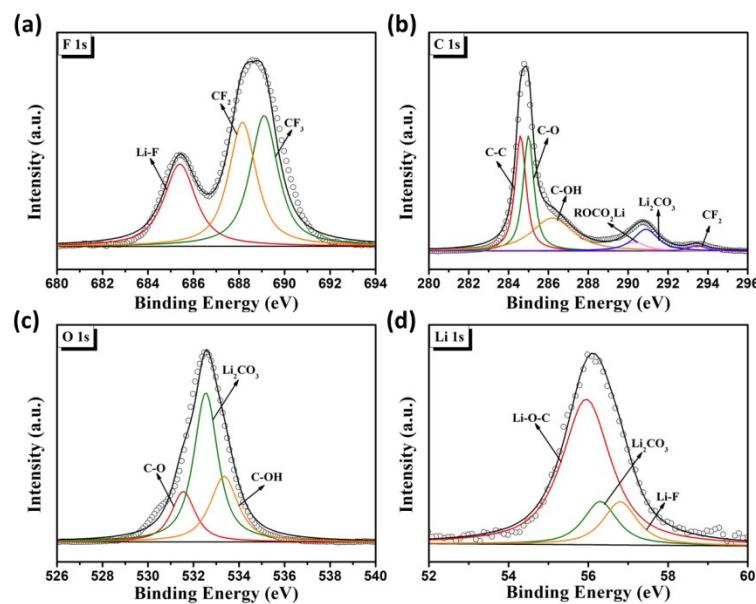
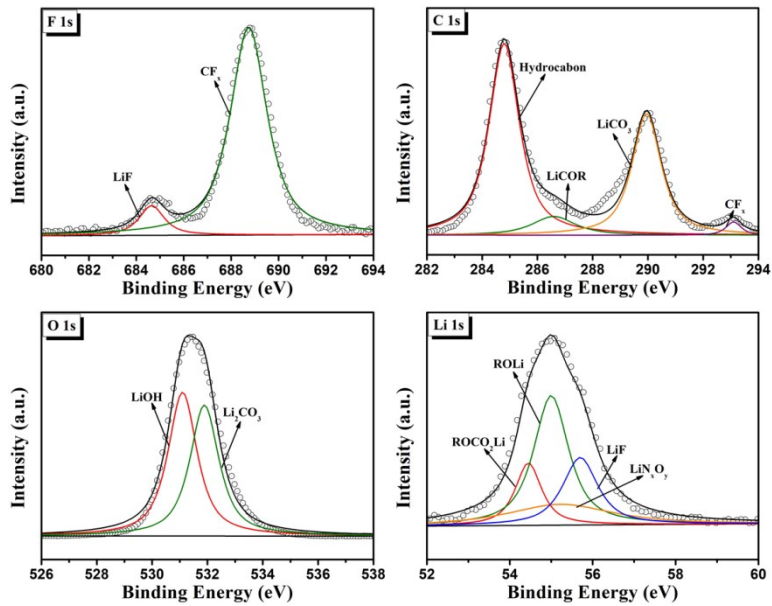
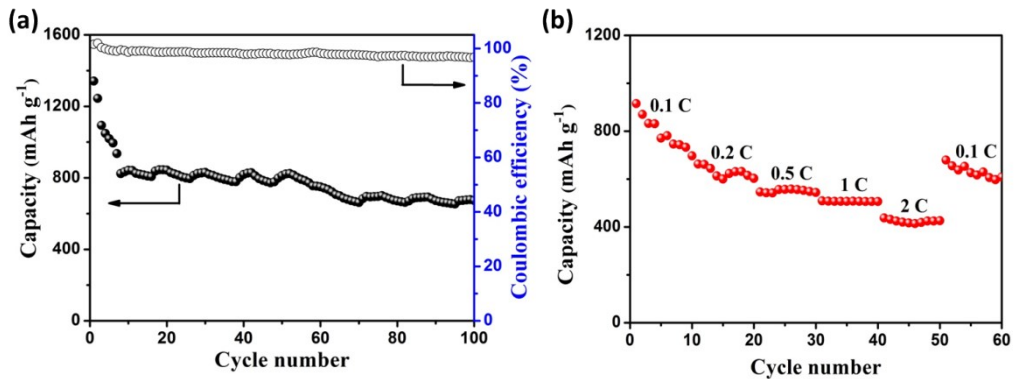


Fig. S6 XPS spectra of MXene@TiO<sub>2</sub>/S cathode surface after cycling: (a) F 1s; (b) C 1s; (c) O 1s; (d) Li 1s.



**Fig. S7** XPS spectra of Li metal anode surface after cycling: (a) F 1s; (b) C 1s; (c) O 1s; (d) Li 1s.



**Fig. S8** (a) Cycling at 0.5 C and (b) rate performances of  $\text{TiO}_2/\text{S}$  cathode.

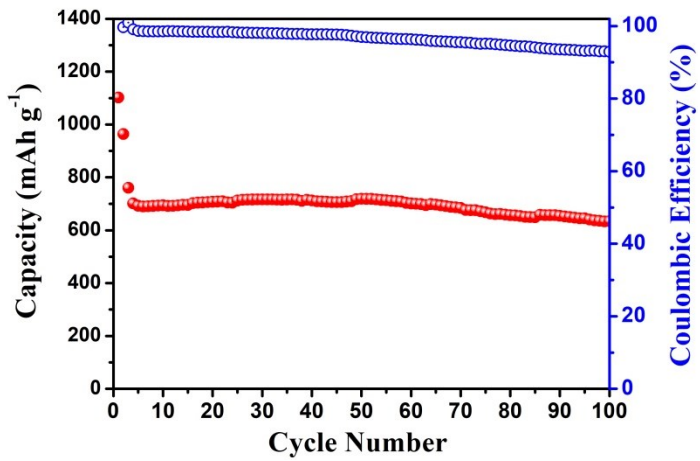


Fig. S9 Cycling behavior at 0.5 C of MXene@TiO<sub>2</sub>/S cathode (sulfur loading=2.5 mg cm<sup>-2</sup>).

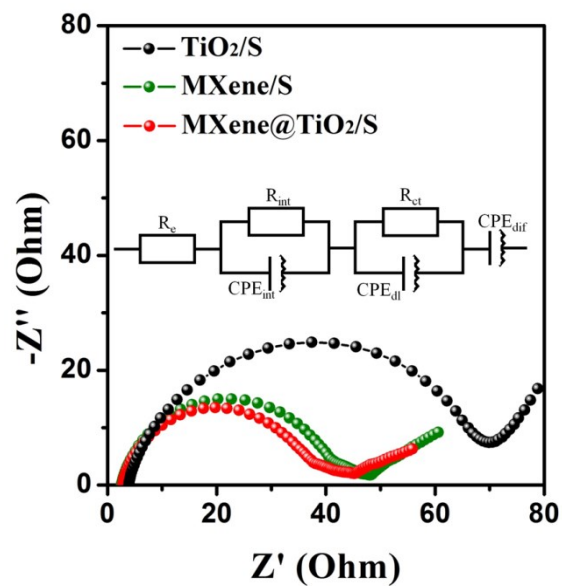


Fig. S10 Nyquist plots of MXene@TiO<sub>2</sub>/S, MXene/S and TiO<sub>2</sub>/S cathodes with the equivalent circuit inset.

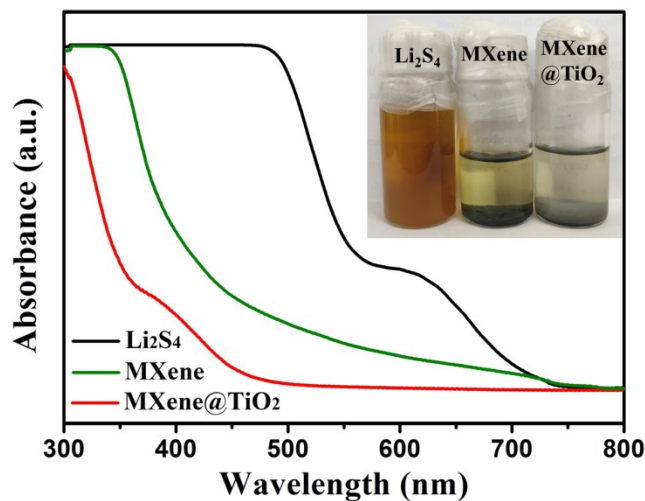


Fig. S11 UV-vis absorption spectra of  $\text{Li}_2\text{S}_4$ , MXene/ $\text{Li}_2\text{S}_4$  and MXene@ $\text{TiO}_2$ / $\text{Li}_2\text{S}_4$  solutions after resting overnight. The digital photo inset shows the consequent color differences.

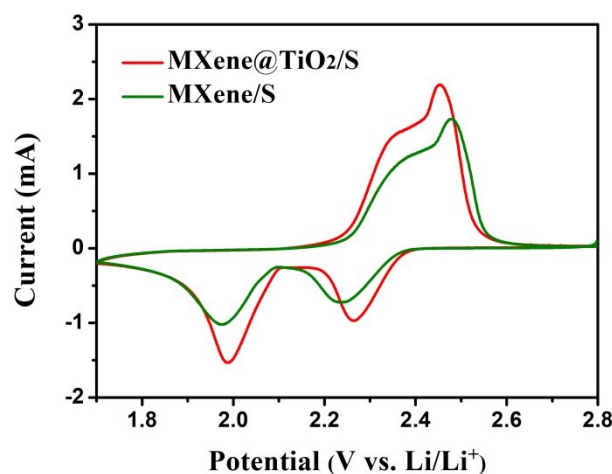


Fig. S12 Comparisons of second-circle CV curves at a scan rate of  $0.2 \text{ mV s}^{-1}$  between MXene@ $\text{TiO}_2$ /S and MXene/S cathodes.

**Table S1.** Elemental composition of MXene@TiO<sub>2</sub> nanoarray based on ICP-OES, C element analysis and stoichiometry.

Samples	C	Ti <sub>(sum)</sub>	Ti <sub>(MXene)</sub>	Ti <sub>(TiO<sub>2</sub>)</sub>
Wt%	6.24	65.13	37.30	27.83

**Table S2.** Electrochemical performance of Li-S batteries based on TiO<sub>2</sub>- and MXene-based hosts.

Host materials	Sulfur (wt%)	Rate (C)	Cycle	Capacity (mAh g <sup>-1</sup> )	Ref.
MXene@TiO <sub>2</sub> nanoarray	71.2	0.5	100	1003.9	This work
MXene@TiO <sub>2</sub> nanoarray	71.2	2	500	612.7	This work
MC-Meso C-doped TiO <sub>2</sub>	61.04	0.1	140	578	1
M2-GC-TiO <sub>2</sub>	59	1	600	599	2
TiO <sub>2</sub> /Ti <sub>2</sub> C	78.4	2	200	464.0	3
GA/TiO <sub>2</sub>	75.1	1	250	512	4
G-TiO <sub>2</sub>	54	0.5	200	853.4	5
Ti <sub>3</sub> C <sub>2</sub> /CNT	79	0.5	1200	450	6
Ti <sub>3</sub> C <sub>2</sub> T <sub>x</sub> /RGO	70.4	0.5	300	878.4	7
Ti <sub>2</sub> C	70	0.5	650	723	8
MXene/1T-2H MoS <sub>2</sub> -C	79.6	0.3	300	799.3	9
N-doped Ti <sub>3</sub> C <sub>2</sub> T <sub>x</sub>	73.85	0.2	200	950	10

**Table S3.** Comparison of EIS fitting results for MXene@TiO<sub>2</sub>/S, MXene/S and TiO<sub>2</sub>/S cathodes.

Cathode materials	R <sub>e</sub> (Ω)	R <sub>int</sub> (Ω)	R <sub>ct</sub> (Ω)
MXene@TiO <sub>2</sub> /S	2.35	7.7	26.8
MXene/S	2.64	8.5	33.8
TiO <sub>2</sub> /S	3.93	32.8	63.9

## **References**

- 1 T. A. Zegeye, C.-F. J. Kuo, A. S. Wotango, C.-J. Pan, H.-M. Chen, A. M. Haregewoin, J.-H. Cheng, W.-N. Su and B.-J. Hwang, *J. Power Source*, 2016, **324**, 239.
- 2 G. D. Park, J. Lee, Y. Piao and Y. C. Kang, *Chem. Eng. J.*, 2018, **335**, 600.
- 3 C. Du, J. Wu, P. Yang, S. Li, J. Xu and K. Song, *Electrochim. Acta*, 2019, **295**, 1067.
- 4 J.-Q. Huang, Z. Wang, Z.-L. Xu, W. G. Chong, X. Qin, X. Wang and J.-K. Kim, *ACS Appl. Mater. Interfaces*, 2016, **8**, 28663.
- 5 H. Fan, Q. Tang, X. Chen, B. Fan, S. Chen and A. Hu, *Chem. Asian J.*, 2016, **11**, 2911.
- 6 X. Liang, Y. Rangom, C. Y. Kwok, Q. Pang and L. F. Nazar, *Adv. Mater.*, 2016, **29**, 1603040.
- 7 W. Bao, X. Xie, J. Xu, X. Guo, J. Song, W. Wu, D. Su and G. Wang, *Chem. Eur J.*, 2017, **23**, 12613.
- 8 X. Liang, A. Garsuch and L. F. Nazar, *Angew. Chem. Int. Ed.*, 2015, **54**, 3907.
- 9 Y. Zhang, Z. Mu, C. Yang, Z. Xu, S. Zhang, X. Zhang, Y. Li, J. Lai, Z. Sun, Y. Yong, Y. Chao, C. Li, X. Ge, W. Yang and S. Guo, *Adv. Funct. Mater.*, 2018, **28**, 1707578.
- 10 W. Bao, L. Liu, C. Wang, S. Choi, D. Wang and G. Wang, *Adv. Energy Mater.*, 2018, **8**, 1702485.